

Variable Contact Angle Model for Gas Hydrate Equilibrium in Porous Media

S. Peddireddy and S.-Y. Lee

Chemical & Natural Gas Engineering, Texas A&M University–Kingsville, Kingsville, TX 78363

J. W. Lee

Dept. of Chemical Engineering, The City College of the City University of New York, New York, NY 10031

DOI 10.1002/aic.10702

Published online October 24, 2005 in Wiley InterScience (www.interscience.wiley.com).

A new thermodynamic model is presented to determine gas hydrate equilibrium in sediments. Using variable contact angles between water and gas in pores, we obtain more accurate prediction of the equilibrium condition of gas hydrates in the sediment than previous studies that used a constant angle of zero. An empirical correlation between variable contact angles and gas solubility is determined in terms of experimental data and is used in the thermodynamic calculations. The new variable contact angle model can reduce the prediction error for equilibrium pressure by more than 50% compared to the Clark–Bishnoi model for temperatures > 274 K. © 2005 American Institute of Chemical Engineers AIChE J, 52: 1228–1234, 2006

Keywords: variable contact angle model, gas hydrate, equilibrium, porous media

Introduction

Gas hydrates are nonstoichiometric compounds formed by the physical combination of water and low molecular weight gases. They are formed when the water molecules form cage-like structures around the gas molecules. Gas hydrates are represented by the general formula $M_n(H_2O)_p$, where M represents the guest gas molecule, n represents the number of guest molecules, and p represents the number of water molecules.¹ Host molecules are held to each other by hydrogen bonds. No chemical attraction exists between the host and guest molecules but a van der Waals force is exerted between them,² except in the case of host molecules containing polar molecules. Gas hydrates are known to exist in one of three structures³: Structure I (sI), Structure II (sII), and Structure H (sH). Structure I (sI) is a body-centered cubic structure; these hydrates are generally present in permafrost regions and in deep oceans. Structure II (sII) is a diamond lattice formed with gases that are bigger than ethane and smaller than pentane.

These hydrates are generally seen in pipeline clogs and in natural gas industries. Each structure forms two types of cavities: pentagonal dodecahedron for a small cavity (sI and sII) and tetrakaidecahedron (sI only) or hexakaidecahedron (sII only) for a large cavity.^{2,3}

Sir Humphrey Davy first discovered gas hydrates in 1811.⁴ Then, interest in the study of hydrates reached its peak in 1934 when the focus of that interest was to solve the problems created by hydrates in the petroleum industry. In the petroleum and natural gas industries, the formation of hydrates is undesirable because the hydrates agglomerate and block pipelines and process equipment, which leads to equipment damage or destruction. However, there are vast deposits of naturally occurring hydrates that contain large amounts of natural gas. According to Collett⁵ and Kenvolden,⁶ it is estimated that nearly 200,000 trillion cubic feet of methane may exist in the form of hydrates in the U.S. permafrost regions and in the surrounding oceans. Later, Milkov⁷ and Klauda and Sandler⁸ refined the global estimation for seafloor gas hydrate using a different method. Several techniques have been proposed to recover the gas from the hydrates: thermal decomposition, depressurization, and slurry mining. However, to evaluate the gas recovery conditions, more accurate study on the formation

Correspondence concerning this article should be addressed to S.-Y. Lee at sangyong.lee@tamuk.edu.

and decomposition of hydrates in porous media is vitally needed.

To recover methane gas from natural gas hydrate deposits, an understanding of the thermodynamic equilibrium of gas hydrates is essential. van der Waals and Platteeuw⁹ developed a statistical thermodynamic model to predict the equilibrium formation conditions of hydrates in a bulk water phase. It was further investigated and modified by Parrish and Praustnitz¹⁰ followed by many other researchers.^{11–15} However, few studies have been done to predict the equilibrium conditions of natural gas hydrates in sediments. Because the equilibrium conditions of gas hydrates in sediments are very different from those in a bulk water phase,^{16,17} a modified thermodynamic model is needed for the hydrate equilibrium in the sediment.

For decades, several thermodynamic models have been developed to predict the gas hydrate equilibrium in sediments. Handa and Stupin¹⁶ were the first to conduct experiments to predict the formation conditions of gas hydrates in sediments. They performed experiments with methane and propane gas in a silica sediment with an average pore size of 70 Å. Uchida et al.¹⁷ experimentally determined the equilibrium conditions for the formation of methane hydrates in glass sediments with pore sizes of 100, 300, and 500 Å. Clarke et al.¹⁸ developed a correlation for the prediction of thermodynamic conditions in sediments based on the assumption that the surface properties (contact angle and surface tension) remain constant and that the pore size of the sediment remains uniform. Their model predicts equilibrium conditions for temperatures between 260 and 274 K for an average pore size of 70 Å, although the error between calculated equilibrium pressure and experimental pressure is >10% at temperatures > 274 K. The error becomes larger with increasing temperature. Klauda and Sandler¹⁹ developed a model in which they used the pore size distribution function to predict the equilibrium instead of using a uniform size. Recently, Turner et al.²⁰ reported that no appreciable shift from the bulk phase equilibrium is found for pore sizes of >600 Å.

A new predictive equilibrium model is presented in this article with the assumption that the contact angle changes as the concentration of gas in the water phase increases. This change of contact angle was already observed by Li and Firoozabadi²¹ in porous media. In this work, the new variable contact angle model is developed and applied to temperatures above the melting point of ice. A correlation between the concentration of gas in water and the contact angle between water and the pore walls is determined. Thus, as the impurity (gas) in the water changes, the surface properties in the pores are determined at each and every equilibrium temperature and pressure.

Thermodynamic Model for Planar Surface

At gas–water–hydrate equilibrium, the chemical potentials of water in the hydrate and in the other coexisting phases are equal.⁹ If liquid water is present, then

$$\mu_w^L(T, P) = \mu_w^H(T, P) \quad (1)$$

where $\mu_w^L(T, P)$ is the water chemical potential of pure liquid and $\mu_w^H(T, P)$ is the water chemical potential of hydrate at temperature T and pressure P .

Using the chemical potential of the empty hydrate lattice (μ^β) as the reference state^{2,10–13} (273.15 K and zero atmospheric pressure), the equilibrium equation becomes

$$\Delta\mu_w^L = \Delta\mu_w^H \quad (2)$$

where $\Delta\mu_w^L = \mu^\beta - \mu_w^L$ and $\Delta\mu_w^H = \mu^\beta - \mu_w^H$.

Calculation of $\Delta\mu_w^H$

The statistical thermodynamic model for the hydrate phase as stated by van der Waals and Platteeuw⁹ is

$$\frac{\Delta\mu_w^H}{RT} = - \sum_{i=1}^2 \nu_i \ln \left(1 - \sum_j \theta_{ij} \right) \quad (3)$$

where ν_i is the number of i -type cavities per water molecule and θ_{ij} is the fractional occupancy of i -type cavities with j -type molecules, expressed as

$$\theta_{ij} = \frac{C_{ij} f_j}{(1 + \sum_j C_{ij} f_j)} \quad (4)$$

where f_j is the fugacity of gas. Herein the Peng–Robinson correlation²² is used for the calculation of the fugacity and C_{ij} is the Langmuir constant. The smooth cell Langmuir¹⁰ coefficient can be calculated as

$$C_{ij} = \frac{1}{kT} \int_0^R 4\pi r^2 \exp \left[- \frac{W_1(r) + W_2(r) + W_3(r)}{kT} \right] dr \quad (5)$$

where $W_1(r)$, $W_2(r)$, and $W_3(r)$ are the smooth cell potentials of the first, second, and third shells and R is the radius of the hydrate cavity,¹¹ which can be calculated using an empirical correlation between the first shell radii of all cavities and the reference chemical potential difference of the theoretical empty hydrate cavity, $\Delta\mu_w^0$, calculated using the distortion model¹²

$$R = \alpha + \beta \times \Delta\mu_w^0 \quad (6)$$

where α , β , and $\Delta\mu_w^0$ are constants, the values of which are listed in Lee and Holder.¹³

Calculation of $\Delta\mu_w^L$

The model developed by Holder et al.²³ is used to predict the chemical potential of water in the aqueous phase that is in equilibrium with the hydrates. The model is given as

$$\frac{\Delta\mu_w^L}{RT_F} = \frac{\Delta\mu_w^0}{RT_0} - \int_{T_0}^{T_F} \frac{\Delta h'_w}{RT^2} dT + \int_0^P \frac{\Delta V'_w}{RT_F} dP - \ln \gamma_w X_w \quad (7)$$

The first term on the right-hand side is the reference chemical potential difference, which is experimentally determined based on the distortion model.^{12,13} The second term gives the temperature dependency of enthalpy at constant pressure. The third

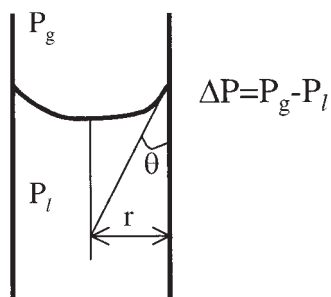


Figure 1. Contact angle in a capillary.

Modified from Clarke et al.¹⁸

term accounts for the change in chemical potential difference arising from pressure. The fourth term gives the activity change of water. The reference properties of sI and sII are available in Lee and Holder.¹³ The temperature dependency of the enthalpy term is given by²

$$\Delta h'_w = \Delta h_w^0 + \int_{T_0}^T \Delta C'_{P_w} dT \quad (8)$$

where Δh_w^0 is an experimentally determined reference enthalpy difference between the empty hydrate lattice and pure water at the reference temperature. $\Delta C'_P$ is the heat capacity difference between the empty hydrate lattice and the water phase, which is a function of temperature, and can be evaluated by the following relationship:

$$\Delta C'_{P_w} = \Delta C_{P_w}^0 + b(T - T_0) \quad (9)$$

where $\Delta C_{P_w}^0$ is a heat capacity experimentally determined at the reference temperature and b is a parameter to fit the experimental data.

Calculation of the Thermodynamic Conditions in Sediments

When gas hydrates are formed in sediments, the equilibrium conditions of gas hydrates mainly depend on the surface properties. The major surface properties include the surface tension and the contact angle. Considering the pores of sediments as small capillary tubes with a uniform radius of r , the pressure difference across the curved surfaces is calculated by the Young–Laplace equation

$$\Delta p = \frac{2\gamma}{r} \quad (10)$$

where Δp is the pressure drop in the capillary tube, γ is the surface tension between the gas and water interface, and r is the radius of the pore as shown in Figure 1.

The activity of water in the pores can be represented as

$$\ln a = -\frac{2\gamma V_l}{RT r} \cos \theta \quad (11)$$

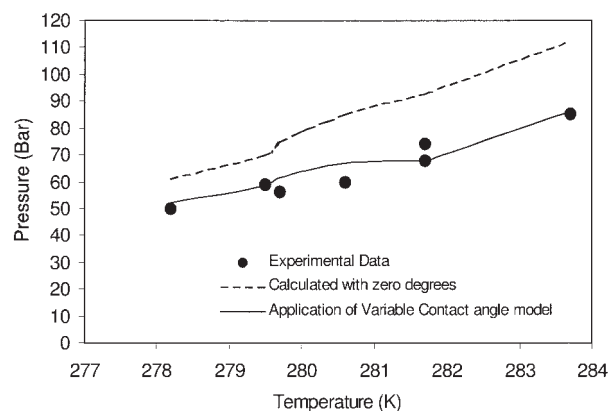


Figure 2. Comparison of equilibrium conditions for a pore size of 300 Å.

where the surface tension is 72.5 dyne/cm.¹⁸ The equation for thermodynamic conditions for the formation of gas hydrates in sediments is given by combining Eqs. 2, 3, 7, and 11:

$$\frac{\Delta \mu_w^0}{RT_0} + \int_{P_0}^{P_l} \frac{\Delta V'_w}{RT_f} dP - \int_{T_0}^{T_f} \frac{\Delta h'_w}{RT^2} dT - \ln \gamma_w X_w + \sum_i \nu_i \ln \left(1 - \sum_j \theta_{ij} \right) = \frac{-2\gamma V_l}{rRT} \cos \theta \quad (12)$$

The following assumptions are made to determine the equilibrium conditions of gas hydrates in the sediment:

(1) The contact angle of water changes as a function of the concentration of gas in water.

Table 1. Comparison of Methane Hydrate Equilibrium in Sediments between the Predicted Equilibrium Data from the Clarke et al. Model and from the New Model

Mean Pore Size (Å)	Temperature (K)	Error(%) [*]	
		From Clarke et al.	From the New Model
50 ^{**}	274	4.62	1.46
	275	4.99	0.24
	276	6.16	2.13
70 [†]	273.2	6.83	0.53
	274.2	5.42	0.69
	276.2	11.83	0.29
119 ^{††}	277.2	10.77	1.08
	277.6	9.85	0.15
	277.7	6.34	1.127
300 ^{**}	278.2	19.81	4.00
	279.5	21.95	1.05
	279.7	20.83	10.00
	280.6	21.91	4.28
	281.7	16.45	0.29
500 ^{**}	283.7	16.57	1.17
	278.5	19.79	2.83
	281.3	16.10	1.50
	281.5	14.40	2.01
	281.6	18.65	2.21

^{*}Error% = $|P_{\text{calculated}} - P_{\text{experiment}}| / P_{\text{experiment}} \times 100\%$.

^{**}Experimental data obtained by Uchida et al.¹⁷

[†]Experimental data obtained by Smith et al.²⁶

^{††}Experimental data of Handa and Stupin.¹⁶

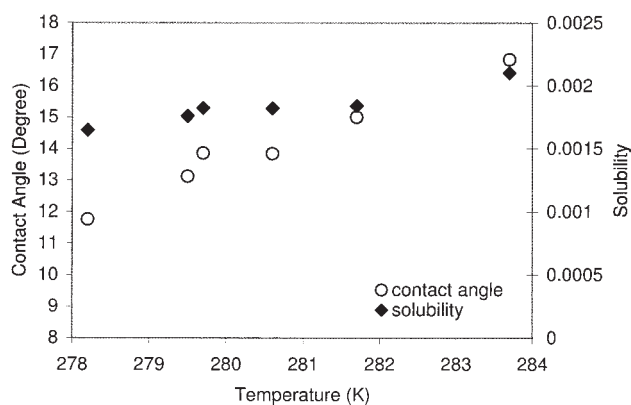


Figure 3. Relationship between contact angle, methane solubility, and equilibrium temperature.

(2) The solubility of gas in water can be calculated using Henry's constant.

(3) This model assumes a uniform pore size.

Determination of contact angle

To determine the contact angle at various conditions, a trial-and-error method has been used. A contact angle is assumed for a corresponding temperature. Then, the pressure is calculated for the corresponding temperature and the assumed contact angle. The calculated pressure based on the contact angle is compared with the experimentally determined pressure. If they are not equal, another angle is assumed and the pressure is recalculated until the analytically determined and experimentally determined pressures are equal for the corresponding temperature. In this manner, all pressures and contact angles are determined in the temperature range from 273.15 to 300 K.

Determination of solubility

The solubility of methane in water is determined using the correlations developed by Chapoy et al.²⁴ The determination of Henry's constant as a function of temperature²⁵ is given by

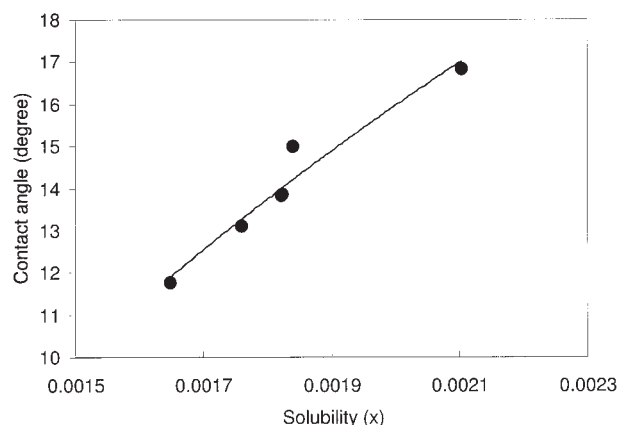


Figure 4. Relationship between contact angle and methane solubility.

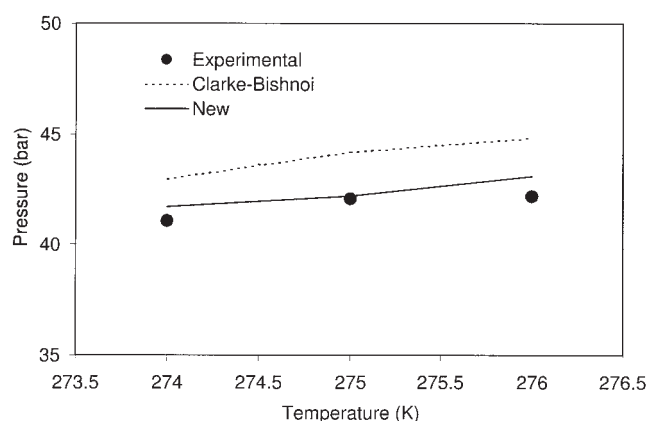


Figure 5. Comparison of equilibrium conditions for a pore size of 50 Å.

$$\log_{10}[H_w^L(T)] = \frac{146.8858 - 5.76834 \times 10^3}{T - 5.19144 \times 10 \log_{10}(T) + 1.84936 \times 10^{-2}T} \quad (13)$$

where T is in degrees Kelvin.

The partial volume of methane is given as a function of temperature in the following equation:

$$V_m(T) = \frac{V_m^\infty(298.15K) V_w^{sat}(T)}{V_w^{sat}(298.15)} \quad (14)$$

The saturation vapor pressure of water is calculated by the following expression:

$$P^{sat} = e^{[A + (B/T)] + C \ln(T) + DT^E} \quad (15)$$

where the values of the coefficients A , B , C , and D are the same as those reported in Chapoy et al.²⁴

Using the above correlations and data, the solubility of methane is given by

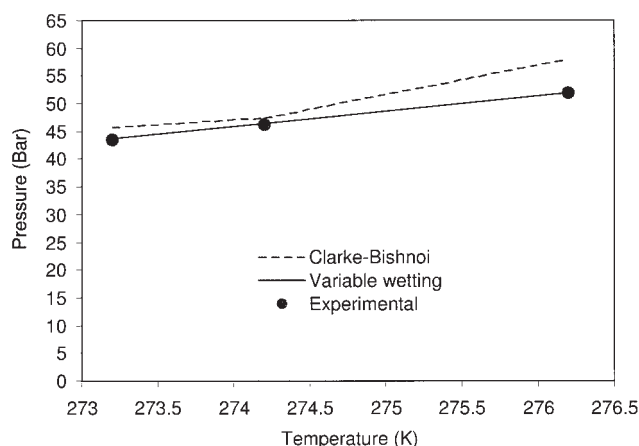


Figure 6. Comparison of equilibrium conditions for a pore size of 70 Å.

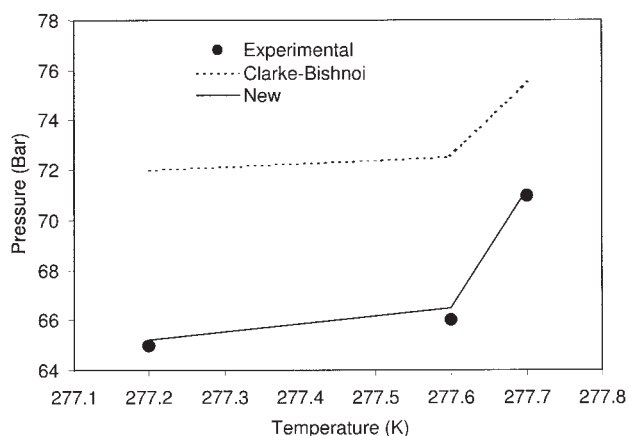


Figure 7. Comparison of equilibrium conditions for a pore size of 119 Å.

$$X_m(T) = \frac{f_j}{H_w^L(T) \exp[V_m^L(T)/(RT)](P - P^{sat})} \quad (16)$$

In this equation f_j is the fugacity of gas, which is determined using the Peng–Robinson equation of state.²²

Results and Discussion

The equilibrium conditions of methane gas hydrate are calculated using the equation proposed by Clarke et al.¹⁸ The data are plotted with pressure on the y-axis and temperature on the x-axis, as shown in Figure 2. The experimental data of Uchida et al.¹⁷ for 300 Å are also shown in Figure 2. The errors between the extrapolated experimental data and the analytically determined data using the model presented by Clarke et al.¹⁸ are shown in Table 1. In terms of the variable contact angle, the errors become smaller at >278 K compared to the error calculated by the Clarke et al. model.¹⁸

Figure 3 shows the methane solubility at hydrate equilibrium pressures with different temperatures in terms of Eqs. 13–16. The solubility of methane in water at each hydrate equilibrium pressure increases as the temperature increases. Thus, the concentration of methane gas in water increases as its solubility increases. According to the work by Firoozabadi and Li,²¹ it

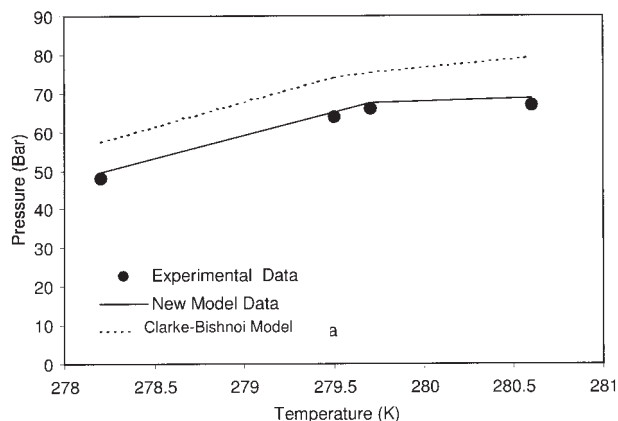


Figure 8. Comparison of equilibrium conditions for a pore size of 500 Å.

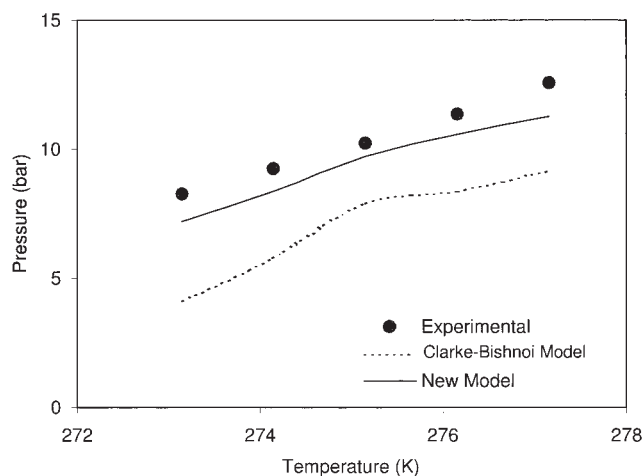


Figure 9. Comparison of equilibrium conditions of ethane hydrate in silica gel with an average pore size of 50 Å.

can be concluded that there is a change in the wetting angle as the concentration of impurities in water increases. Figure 3 shows the relationship between the iteratively determined wetting angle and the temperature to fit the experimental data by Uchida et al.¹⁷ From Figure 3, it is shown that the wetting angle increases as the temperature increases. The solubility data calculated at the equilibrium temperature and pressure are plotted against the wetting angle as shown in Figure 4. A trend line is drawn between the wetting angle and the solubility and is given as

$$\theta = 21.015 \ln(X_m) + 146.56 \quad (17)$$

The contact angle is an implicit function of equilibrium temperature and pressure because it is related to the methane solubility (X_m). Figure 2 shows the calculation result of using a variable contact angle for the equilibrium calculation of methane gas hydrate in sediments with an average pore size of 300 Å. Table 1 shows that the new variable contact angle model gives a more accurate prediction than the results ob-

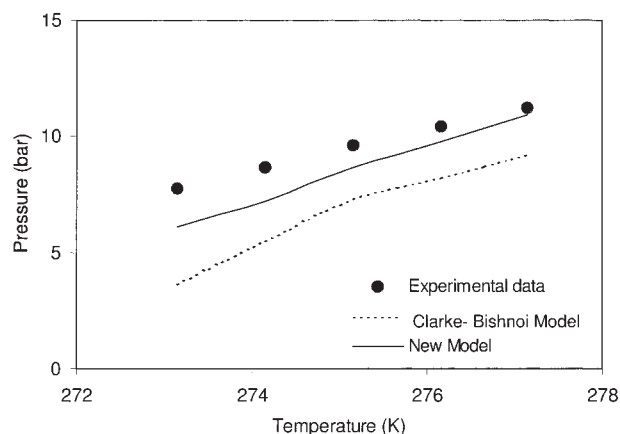


Figure 10. Comparison of equilibrium conditions of ethane hydrate in silica gel with an average pore size of 75 Å.

Table 2. Comparison of Ethane Hydrate Equilibrium in Sediments between the Predicted Equilibrium Data from the Clarke et al. Model and from the New Model

Mean Pore Size (Å)	Temperature (K)	Error(%) [*]	
		From Clarke et al.	From the New Model
50**	273.2	50.42	12.82
	274.2	37.37	9.83
	275.2	22.93	5.07
	276.2	26.41	6.95
	277.2	27.09	10.12
75**	273.2	53.43	21.09
	274.2	36.34	16.67
	275.2	24.04	10.09
	276.2	21.46	6.61
	277.2	17.93	2.76

^{*}Error% = $|P_{\text{calculated}} - P_{\text{experimental}}| / P_{\text{experimental}} \times 100\%$.

^{**}Experimental data of Zhang et al.²⁷

tained by Clarke et al.,¹⁸ especially as the temperature increases.

We also apply this variable contact angle model to determine the equilibrium conditions for methane hydrates in glass sediments of pore sizes 50, 70, 119, and 500 Å in Figures 5, 6, 7, and 8 (Table 1), respectively. A comparison between the experimental data by Smith et al.²⁶ and the predicted equilibrium conditions using the two different methods is shown in Figure 5. Figure 6 shows a comparison between the results from the new variable contact model and the Clarke et al. model (zero contact angle) with reference to Handa and Stupin's experimental data.¹⁶ Figures 7 and 8 compare the experimental data reported by Uchida et al.¹⁷ with the calculated results by the Clarke et al. equation¹⁸ and the calculated results by the variable contact angle model. Table 1 together with Figures 5 to 8 show that the new predictive model gives better results than the zero-degree contact angle method when compared to the experimental data.

In Figures 9 and 10, the equilibrium conditions of ethane gas hydrate in sediments with an average pore size of 50 and 75 Å have been calculated using Eq. 17. As shown in Figures 9 and 10, the error between predicted data and experimental data for ethane gas hydrate was reduced to less than half. This shows that the model may have the potential to be used as a general model. The solubility of ethane gas in water is determined using Henry's constant.² Table 2 shows that the new contact angle model substantially reduces the errors compared to the zero contact angle model.

Conclusions

A new model with variable contact angles between water and gas in pores has been developed to predict the gas hydrate equilibrium in porous media at temperatures above the ice melting point. In the new model, a contact angle is calculated using the empirical correlation between the solubility of methane gas in water and the contact angle of water in sediments with an average pore size of 300 Å. After applying the empirical model to the calculation of the hydrate equilibrium of methane gas in sediments with average pore sizes of 50, 70, 119, and 500 Å, the percentage error between calculated equilibrium pressure and experimental equilibrium pressure is reduced by more than half. We also apply the model to the

prediction of ethane gas hydrate in sediments with average pore sizes of 50 and 75 Å and reduce the prediction error. By applying various pore size distribution functions to the new model, more accurate prediction of the equilibrium conditions can be made in the future.

Acknowledgments

The corresponding author is grateful for the support of American Chemical Society–Petroleum Research Fund for summer research at the City College of New York.

Notation

A, B, C, D = coefficients defined in Eq. 15

C_{ij} = Langmuir constant, kPa^{-1}

ΔC_{P_w} = molar heat capacity difference between the empty hydrate lattice and pure water phase, $\text{J mol}^{-1} \text{K}^{-1}$

f = fugacity

Δh_w^0 = molar enthalpy difference between the empty hydrate lattice and pure water at 273.15 K and 0 atm, J/mol

P = pressure, bar ($=10^5 \text{ Pa}$)

ΔP = pressure difference in a capillary tube, bar

R = gas constant

r = radius of pore

T = temperature

V_1 = volume, m^3

V_m, V_w = methane and water partial volume, m^3/mol

ΔV_w = water volume difference between the empty hydrate lattice and pure water phase, m^3/mol

W_1, W_2, W_3 = cell potential for first, second, and third shell, kJ/mol

X_m, X_w = mole fractions of methane and water

Greek letters

α, β = coefficients defined in Eq. 6

γ = surface tension

γ_w = activity coefficient of water

$\Delta \mu_w^0$ = difference of chemical potential of water and theoretical empty hydrate at 273.15 K and 0 pressure, J/mol

$\Delta \mu_w^L$ = difference between the chemical potential of water in the unoccupied hydrate lattice and the bulk water phase, J/mol

$\Delta \mu_w^H$ = difference between the chemical potential of water in the unoccupied hydrate lattice and the occupied hydrate, J/mol

μ^β = chemical potential of water in the unoccupied hydrate lattice, J/mol

v_i = ratio of small or large cavities to water molecules in a unit cell

θ = degree of contact angle

θ_{ij} = fraction of i -type cavities occupied by j -type gas molecules

Literature Cited

- Lee SY, Holder GD. Methane hydrate: Potential as a future energy source. *Fuel Process Technol.* 2001;71:181-186.
- Holder GD, Zetts SP, Pradhan N. Phase behavior in systems containing clathrate hydrates. *Rev Chem Eng.* 1988;5:1-70.
- Sloan ED Jr. *Clathrate Hydrates of Natural Gases*. 2nd Edition. New York, NY: Marcel Dekker; 1998.
- Davy H. The Bakerian lecture. On some of the combinations of oxymuriatic gas and oxygen, and on the chemical relations of these principles to inflammable bodies. *Philos Trans R Soc Lond.* 1811;101:1-35.
- Office of Fossil Energy, U.S. Department of Energy (US DOE). *Natural Methane Hydrate Multi-Year R&D Program*. Washington, DC: US DOE; 1999.
- Kvenvolden KA. Potential effects of gas hydrate on human welfare. *Proc Natl Acad Sci USA.* 1999;96:3420-3426.
- Milkov AV. Global estimates of hydrate-bound gas in marine sediments: How much is really out there? *Earth-Sci Rev.* 2004;66:183-197.
- Klauda JB, Sandler SI. Global distribution of methane hydrate in ocean sediment: Present and past. *Energy Fuels.* 2005;19:459-470.

9. van der Waals JH, Platteeuw JC. Clathrate solutions. *Adv Chem Phys.* 1959;2:1-57.
10. Parrish WR, Prausnitz JM. Dissociation pressure of gas hydrates formed by gas mixtures. *Ind Eng Chem Process Des Dev.* 1972;11:26-34.
11. John VT, Papadopoulos KD, Holder GD. A generalized model for predicting equilibrium conditions for gas hydrates. *AIChE J.* 1985;31:252-259.
12. Zele SR, Lee SY, Holder GD. A theory of lattice distortion in gas hydrates. *J Phys Chem B.* 1999;43:10250-10257.
13. Lee SY, Holder GD. Model for gas hydrate equilibria using a variable reference chemical potential: Part 1. *AIChE J.* 2002;48:161-167.
14. Bazant MZ, Trout BL. A method to extract potentials from the temperature dependence of Langmuir constants for clathrate hydrates. *Physica A.* 2001;300:139-173.
15. Ballard AL, Sloan ED Jr. The next generation of hydrate prediction. I. Hydrate standard states and incorporation of spectroscopy. *Fluid Phase Equilib.* 2002;194/197:371-384.
16. Handa YP, Stupin DJ. Thermodynamic properties and dissociation characteristic of methane and propane hydrates in 70-Å-radius silica gel pores. *Phys Chem.* 1992;96:8599-8603.
17. Uchida T, Ebinuma T, Ishizaki T. Dissociation condition measurements of methane hydrate in confined small pores of porous glass. *J Phys Chem B.* 1999;103:3659-3662.
18. Clarke MA, Pooladi-Darvish M, Bishnoi PR. A method to predict equilibrium conditions of gas hydrate formation in porous media. *Ind Eng Chem Res.* 1999;38:2485-2490.
19. Klauda JB, Sandler SI. Modeling natural gas hydrate phase equilibria in laboratory and natural porous media. *Ind Eng Chem Res.* 2001;40:4197-4208.
20. Turner DJ, Cherry RS, Sloan ED. Sensitivity of methane hydrate phase equilibria to sediment pore size. *Fluid Phase Equilib.* 2004;228/229:505-510.
21. Li K, Firoozabadi A. Experimental study of wettability alteration to preferential gas-wetness in porous media and its effect. *SPEREE.* 2000;April:139-149.
22. Peng DY, Robinson DB. A new two-constant equation of state. *Ind Eng Chem Fundam.* 1976;15:59-64.
23. Holder GD, Corbin G, Papadopoulos KD. Thermodynamic and molecular properties of gas hydrates containing methane, argon and krypton. *Ind Eng Chem Fundam.* 1980;19:282-286.
24. Chapoy A, Coquelet C, Richon D. Solubility measurement and modeling of water in the gas phase of the methane/water binary system at temperatures from 283.08 to 318.12 K and pressures up to 34.5 MPa. *Fluid Phase Equilib.* 2003;214:101-117.
25. Yaws CL, Hopper JR, Wang X, Rathinsamy AK, Pike RW. Calculating solubility and Henry's law constants for gases in water. *Chem Eng.* 1999;June:102-105.
26. Smith DH, Wilder JW, Seshadri K. Methane hydrate equilibria in silica gels with broad pore-size distributions. *AIChE J.* 2002;48:393-400.
27. Zhang W, Wilder JW, Smith DH. Interpretation of ethane hydrate equilibrium data for porous media involving hydrate-ice equilibria. *AIChE J.* 2002;48:2324-2331.

Manuscript received Dec. 7, 2004, and revision received Aug. 30, 2005.